

Direct controller order reduction by identification in closed loop applied to an active suspension

I. D. Landau[†], A. Constantinescu[†], A. Karimi[‡]

[†] Laboratoire d'Automatique de Grenoble
 ENSIEG, BP 46
 38402 Saint Martin d'Hères
 e-mail: landau@lag.ensieg.inpg.fr

[‡] Electrical Engineering Department, Sharif University of Technology
 Azadi Ave., Teheran Iran;
 e-mail: karimi@sina.sharif.ac.ir

Abstract

After briefly reviewing some algorithms for direct controller order reduction by identification in closed loop using simulated and real data, validation tests are proposed. Then the methodology is illustrated by its application to controller order reduction for an active suspension system. Experimental results are presented.

Keywords : Controller reduction, Closed loop identification, Active suspension

1 Introduction

In this paper we will focus on the use of closed loop identification techniques for direct controller order reduction. One of the basic bloc diagram for reduced order controller identification is shown in Fig. 1 (input matching scheme). The upper part represents the sim-

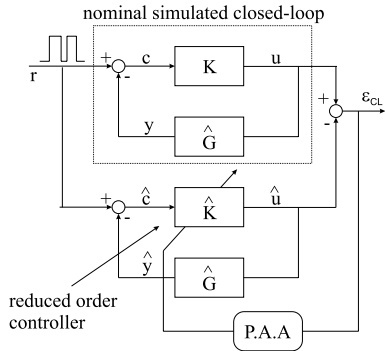


Figure 1: Closed-loop identification of reduced order controllers using simulated data(input matching)

ulated nominal closed loop system. It is constituted by the nominal designed controller (denoted by K) and the best identified plant model (i.e. which leads to the closest behaviour of the true closed loop system and of the nominal simulated one) denoted by \hat{G} .

The lower part is constituted by the estimated reduced

order controller (denoted by \hat{K}) in feedback connection with the plant model used in the simulation of the nominal system. The parametric adaptation algorithm will try to find the best reduced order controller of a given order which will minimize the closed loop input error expressed as the difference between the input of the plant model generated in the nominal simulated closed loop and the input of the plant model generated by the closed loop using the reduced order controller (i.e. which will minimize the discrepancy between the two closed loops).

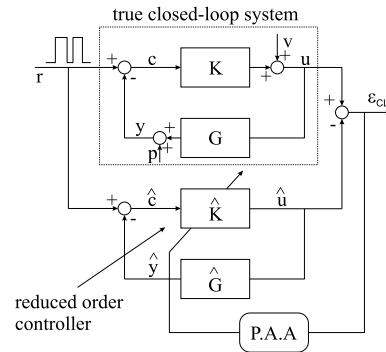


Figure 2: Closed-loop identification of the reduced order controllers using real data (input matching)

However one can consider as an objective for controller order reduction to minimize the closed loop error between the plant output generated in the nominal simulated closed loop and the plant output generated by the closed loop using the reduced order controller. This can be achieved using the scheme of Fig. 1 but filtering the external excitation r through \hat{G} .

Identification of a reduced order controller can also be done by using real data as shown in Fig. 2 (the upper part represents the true closed loop system). Note that the adjustable closed loop predictor (lower part) may use a plant model identified in closed-loop with the nominal controller or more precisely the plant model available

which gives the best results when a ‘‘closed loop’’ model validation test is used (see [3, 1]).

The paper is organized as follows. In Section 2 the recursive algorithms for direct identification of the reduced order controllers will be reviewed. The validation of the estimated reduced order controller will be discussed in Section 3. The active suspension system is presented in Section 4, the experimental results concerning the identification of reduced order controllers for the active suspension being given in Section 5. Finally we will have some concluding remarks.

2 Algorithms for direct closed loop identification of reduced order controllers

We will often make reference to [5, 2, 4] for details of the algorithms and proofs.

2.1 Algorithms

Consider the upper part of Fig. 1. The nominal simulated closed loop is formed by the estimated plant model and the nominal controller. The estimated plant model is defined by the transfer operator:

$$\hat{G}(q^{-1}) = \frac{q^{-d}\hat{B}(q^{-1})}{\hat{A}(q^{-1})} \quad (1)$$

where:

$$\begin{aligned} \hat{B}(q^{-1}) &= \hat{b}_1 q^{-1} + \dots + \hat{b}_{n_B} q^{-n_B} \\ &= q^{-1} \hat{B}^*(q^{-1}) \end{aligned} \quad (2)$$

$$\begin{aligned} \hat{A}(q^{-1}) &= 1 + \hat{a}_1 q^{-1} + \dots + \hat{a}_{n_A} q^{-n_A} \\ &= 1 + q^{-1} \hat{A}^*(q^{-1}). \end{aligned} \quad (3)$$

The plant model is operated in closed loop with a digital controller:

$$K = \frac{R(q^{-1})}{S(q^{-1})} \quad (4)$$

with:

$$R(q^{-1}) = r_0 + r_1 q^{-1} + \dots + r_{n_R} q^{-n_R} \quad (5)$$

$$S(q^{-1}) = 1 + s_1 q^{-1} + \dots + s_{n_S} q^{-n_S} \quad (6)$$

$$= 1 + q^{-1} S^*(q^{-1}) \quad (7)$$

$u(t)$ is the plant input, $y(t)$ is the plant output and $r(t)$ is the external excitation signal (eventually filtered).

The output of the nominal controller is given by:

$$u(t+1) = -S^*(q^{-1})u(t) + R(q^{-1})c(t+1) \quad (8)$$

$$= \theta^T \psi(t) \quad (9)$$

where

$$c(t+1) = r(t+1) - y(t+1) \quad (10)$$

$$y(t+1) = -\hat{A}^* y(t) + \hat{B}^* u(t-d) \quad (11)$$

$$\begin{aligned} \psi^T(t) &= [-u(t), \dots, -u(t-n_S+1), \\ & c(t+1), \dots, c(t-n_R+1)] \end{aligned} \quad (12)$$

$$\theta^T = [s_1, \dots, s_{n_S}, r_0, \dots, r_{n_R}] \quad (13)$$

The output of the estimated reduced order controller (of orders $n_{\hat{S}}$ and $n_{\hat{R}}$) is given by (see the lower part of Fig. 1):

a priori:

$$\hat{u}^0(t+1) = \hat{\theta}^T(t) \phi(t) \quad (14)$$

a posteriori:

$$\hat{u}(t+1) = \hat{\theta}^T(t+1) \phi(t) \quad (15)$$

where :

$$\begin{aligned} \hat{\theta}^T(t) &= [\hat{s}_1(t), \dots, \hat{s}_{n_{\hat{S}}}(t), \\ & \hat{r}_0(t), \dots, \hat{r}_{n_{\hat{R}}}(t)] \end{aligned} \quad (16)$$

$$\begin{aligned} \phi^T(t) &= [-\hat{u}(t), \dots, -\hat{u}(t-n_{\hat{S}}+1), \\ & \hat{c}(t+1), \dots, \hat{c}(t-n_{\hat{R}}+1)] \end{aligned} \quad (17)$$

$$\hat{c}(t+1) = r(t+1) - \hat{y}(t+1) \quad (18)$$

$$= r(t+1) + \hat{A}^* \hat{y}(t) - \hat{B}^* \hat{u}(t-d) \quad (19)$$

Closed loop input matching algorithm (CLIM)

The closed loop input error is given by:

a priori:

$$\varepsilon_{CL}^0(t+1) = u(t+1) - \hat{u}^0(t+1) \quad (20)$$

a posteriori:

$$\varepsilon_{CL}(t+1) = u(t+1) - \hat{u}(t+1) \quad (21)$$

and the parameter adaptation algorithm will be given by:

$$\hat{\theta}(t+1) = \hat{\theta}(t) + F(t) \Phi(t) \varepsilon_{CL}(t+1) \quad (22)$$

$$\begin{aligned} F^{-1}(t+1) &= \lambda_1(t) F^{-1}(t) \\ &+ \lambda_2(t) \Phi(t) \Phi^T(t) \end{aligned} \quad (23)$$

$$0 < \lambda_1(t) \leq 1 \quad ; \quad 0 \leq \lambda_2(t) < 2; \quad F(0) > 0$$

$$\varepsilon_{CL}(t+1) = \frac{u(t+1) - \hat{u}^0(t+1)}{1 + \Phi^T(t) F(t) \Phi(t)} \quad (24)$$

Specific algorithms will be obtained by an appropriate choice of the observation vector $\Phi(t)$ as follows:

CLIM

$$\Phi(t) = \phi(t)$$

F-CLIM

$$\Phi(t) = \frac{\hat{A}(q^{-1})}{\hat{P}(q^{-1})} \phi(t)$$

where:

$$\hat{P}(q^{-1}) = \hat{A}(q^{-1}) S(q^{-1}) + q^{-d} \hat{B}(q^{-1}) R(q^{-1}) \quad (25)$$

Closed loop output matching algorithm (CLOM)

The objective is to create a closed loop error which reflects the difference between the output $y(t)$ of the nominal closed loop simulated system and the output $\hat{y}(t)$ of the simulated closed loop system using the reduced order controller. The corresponding algorithm is obtained using the CLIM algorithms but filtering first $r(t)$ by \hat{G} . The algorithm will minimize the closed loop output error instead of the closed loop input error.

Imposing constraints on the reduced order controllers

Without difficulty fixed parts (filters) can be forced in the reduced order controllers (like integrators, opening of the loop at $0.5f_s$, fixed filters etc.). For this the nominal controller is factorized as $K = K_F K'$ and the reduced order controller is factorized as $\hat{K} = K_F \hat{K}'$ where K_F corresponds to the fixed part of the controller which we would like to be contained in the reduced order controller.

2.2 Properties of the estimated controllers (Bias analysis)

We will summarize next the asymptotic properties of the estimated controller (characterized by the parameter vector $\hat{\theta}^*$) corresponding to the various algorithms when using simulated and real-time data [5, 4].

Closed loop input matching algorithms

a) Use of simulated data

The asymptotic bias distribution of the parameter estimates in the frequency domain will be given by :

$$\begin{aligned}\hat{\theta}^* &= \arg \min_{\theta} \int_{-\pi}^{\pi} |\hat{S}_{yp}|^2 |K - \hat{K}|^2 |\hat{S}_{yp}|^2 \phi_r(\omega) d\omega \\ &= \arg \min_{\theta} \int_{-\pi}^{\pi} |\hat{S}_{up} - \hat{S}_{up}|^2 \phi_r(\omega) d\omega\end{aligned}\quad (26)$$

where $\hat{\theta}^*$ is the vector of estimated parameters of the reduced order controller and ϕ_r is the spectral density of the excitation signal and

$$\hat{S}_{yp}(q^{-1}) = \frac{1}{1 + K\hat{G}} = \frac{\hat{A}(q^{-1})S(q^{-1})}{\hat{P}(q^{-1})}\quad (27)$$

$$\hat{S}_{yp}(q^{-1}) = \frac{1}{1 + \hat{K}\hat{G}} = \frac{\hat{A}(q^{-1})\hat{S}(q^{-1})}{\hat{P}(q^{-1})}\quad (28)$$

$$\hat{S}_{up}(q^{-1}) = -\frac{K}{1 + K\hat{G}} = -\frac{\hat{A}(q^{-1})R(q^{-1})}{\hat{P}(q^{-1})}\quad (29)$$

$$\hat{S}_{up}(q^{-1}) = -\frac{\hat{K}}{1 + \hat{K}\hat{G}} = -\frac{\hat{A}(q^{-1})\hat{R}(q^{-1})}{\hat{P}(q^{-1})}\quad (30)$$

with:

$$\hat{P}(q^{-1}) = \hat{A}(q^{-1})\hat{S}(q^{-1}) + q^{-d}\hat{B}(q^{-1})\hat{R}(q^{-1})\quad (31)$$

This expression clearly shows that:

- The two norm of the difference between \hat{S}_{up} and \hat{S}_{up} is minimized when $r(t)$ is a white noise signal.

- The frequency distribution of the error between the two controllers is weighted by the spectrum of the output sensitivity function of the nominal simulated system and the spectrum of the estimated output sensitivity function (given by the plant model and the estimated reduced order controller).
- The frequency distribution of the bias can be tuned by the choice of $r(t)$.

Like in the plant model identification in closed loop, the error in the frequency domain between the two controllers will be small in the critical frequency regions for control. This can be further adjusted by the use of an appropriate excitation signal.

b) Use of real data

The asymptotic bias distribution of the parameters estimates in the frequency domain will be given by:

$$\begin{aligned}\hat{\theta}^* &= \arg \min_{\theta} \int_{-\pi}^{\pi} |S_{up} - \hat{S}_{up}|^2 \phi_r(\omega) \\ &+ |S_{yp}|^2 \phi_{v'}(\omega) d\omega\end{aligned}\quad (32)$$

where

$$S_{up}(q^{-1}) = -\frac{K}{1 + KG} = -\frac{A(q^{-1})R(q^{-1})}{P(q^{-1})}\quad (33)$$

$$P(q^{-1}) = A(q^{-1})S(q^{-1}) + q^{-d}B(q^{-1})R(q^{-1})\quad (34)$$

and

$$v'(t) = v(t) - Kp(t)\quad (35)$$

This expression shows that:

- The noise does not affect estimation of the controller parameters.
- When using real data, the closed loop system with reduced order controller approximates the real closed loop system instead of the nominal one.

Closed loop output matching (CLIM with filtered r)

a) Simulated data

The asymptotic bias distribution of the parameter estimates in the frequency domain will be given by:

$$\begin{aligned}\hat{\theta}^* &= \arg \min_{\theta} \int_{-\pi}^{\pi} |\hat{S}_{yp}|^2 |K - \hat{K}|^2 |\hat{S}_{yv}|^2 \phi_r(\omega) d\omega \\ &= \arg \min_{\theta} \int_{-\pi}^{\pi} |\hat{S}_{yp} - \hat{S}_{yp}|^2 \phi_r(\omega) d\omega\end{aligned}\quad (36)$$

where $\hat{\theta}^*$ is the vector of estimated parameters of the reduced order controller and ϕ_r is the spectral density of the excitation signal, \hat{S}_{yp} , \hat{S}_{yv} are defined in the equations (27) and (28) respectively and

$$\hat{S}_{yv}(q^{-1}) = \frac{\hat{G}}{1 + \hat{K}\hat{G}} = \frac{q^{-d}\hat{B}(q^{-1})\hat{S}(q^{-1})}{\hat{P}(q^{-1})}\quad (37)$$

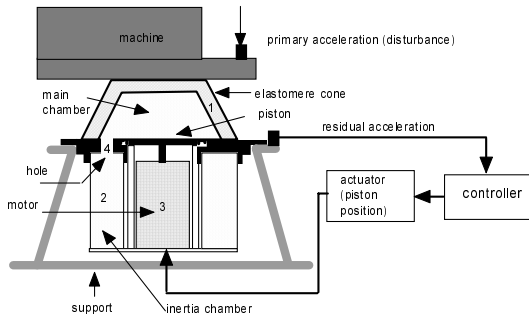


Figure 3: The active suspension system

- The two norm expression of the difference between \hat{S}_{yp} and \hat{S}_{yp} is minimized when $r(t)$ is a white noise signal.
- The frequency distribution of the bias is weighted by the spectrum of the output sensitivity function of the nominal simulated system and the spectrum of the estimated sensitivity function with respect to an input disturbance (given by the plant model and the estimated reduced order controller).
- The frequency distribution of the bias can be tuned by the choice of $r(t)$.

b) Use of real data

The asymptotic bias distribution will be given by Eq. (32) in which $\phi_r(\omega)$ is replaced by $|\hat{G}|^2 \phi_r(\omega)$.

3 Validation of the estimated reduced order controller

Case a) Simulated Data

The resulting reduced order controller should stabilize the nominal model and should give sensitivity functions which are close to the nominal ones in the critical frequency regions for performance and robustness.

The Vinnicombe distance (ν -gap)[7] between the sensitivity functions obtained with the nominal and with the reduced order controller gives useful information about their closeness.

Comparing also visually the frequency characteristics of the various sensitivity functions is important.

A possible validation test is to use the dual Vinnicombe stability test (sufficient condition) [7].

Case b) Real-time data

In this case one has in addition the option to take advantage of the available real-time data.

With reference to Fig. 2 the objective is to test to what extent the estimated closed loop with a reduced order controller is close to the real closed loop system formed by the plant and the nominal controller.

A basic information is provided by the variance of the residual closed loop error.

The other alternative which seems very interesting is to compute the Vinnicombe gap between the transfer function of the true closed loop system which uses the nominal controller (obtained by input/output identification between r and u) and the computed transfer function of the closed-loop formed by the reduced order controller and the estimated plant model.

4 The active suspension

The procedure for obtaining reduced order controllers by identification in closed loop will be illustrated for the case of the control of an active suspension. The active suspension is shown in Fig. 3 and the corresponding block diagram in Fig. 4. The controller through the power amplifier will act upon the piston in order to reduce the residual acceleration. The frequency spectrum of the vibrations which have to be reduced is limited by an upper frequency lower than 200 Hz. The system is controlled by a PC via an I/O board. The sampling frequency is 800 Hz.

The primary acceleration has been generated using a shaker. Its input is a signal given by the computer. The frequency characteristic of the identified primary path model, between the excitation of the shaker and the residual acceleration is presented in figure 5. The goal is to compute a controller which minimizes the residual acceleration around the first vibration mode and tries to distribute the amplification of the disturbances over the high frequency range. There exist several vibration modes (see figure 5), the first one being at $31.47Hz$ with a damping factor 0.093.

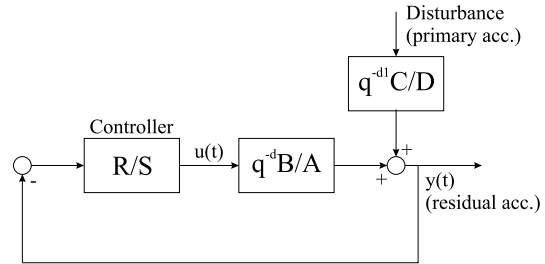


Figure 4: Block diagram of the active suspension system

The identified plant model, between the piston's position and the residual acceleration (the secondary path), has the following complexity: $n_B = 11$, $n_A = 12$, $d = 2$. The system contains a double derivator. In Fig. 6 are presented the frequency characteristics of two plant models: the open loop identified model used for design and the model identified in closed loop using the nominal controller. The closed loop identified model provided better closed loop validation results.

Both models give close results for controller reduction despite their differences in terms of closed loop validation. However for the remaining of the paper, the results are given for the model identified in closed loop.

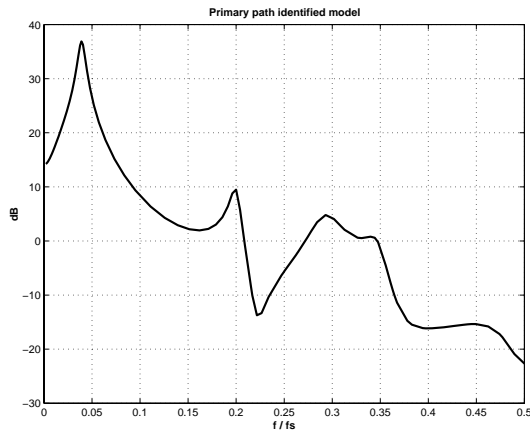


Figure 5: The frequency characteristic of the primary path model (input: shaker’s signal, output: residual acceleration)

The model has six vibration modes. Five of the six vibration modes have a very low damping (< 0.085).

Note that an important attenuation on S_{yp} is required at the frequency of the first vibration mode.

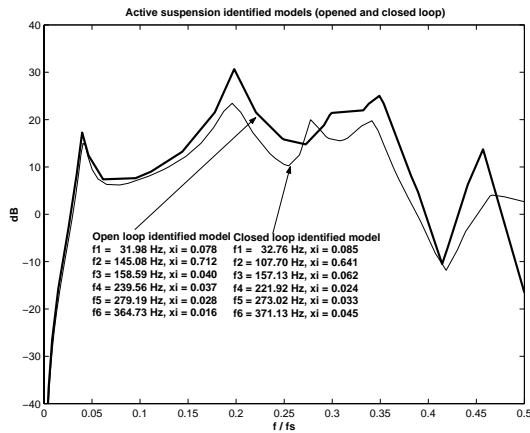


Figure 6: The frequency characteristics of the secondary path model (input: piston displacement, output: residual acceleration)

The nominal controller has been designed using the method of “pole placement with sensitivity function shaping by convex optimization” [6]. A pair of dominant poles has been fixed at the frequency of the first vibration mode and with a damping $\xi = 0.8$. In addition a fixed part $H_R = 1 + q^{-1}$ has been introduced in the controller ($R = H_R R'$) which assures the opening of the loop at $0.5 f_s$. The resulting nominal controller satisfying the specifications on the residual acceleration has been obtained. Its complexity is given by the orders of polynomial R and S : $n_R = 27, n_S = 28$. Note that if standard pole placement is used, by solving the Bezout equation it will result a controller having the orders: $n_R = 12, n_S = 13$ (considering the fixed part H_R).

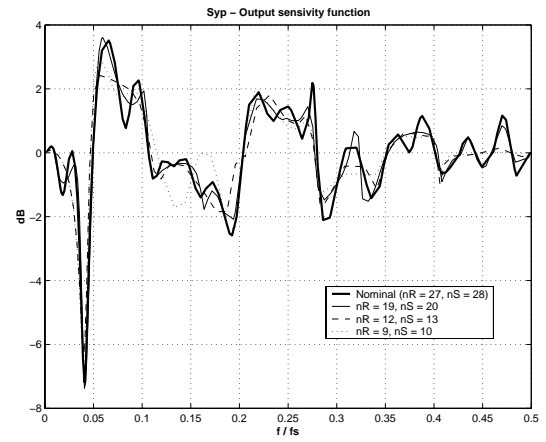


Figure 7: Output sensitivity for the active suspension (controller reduction using CLIM algorithm on simulated data)

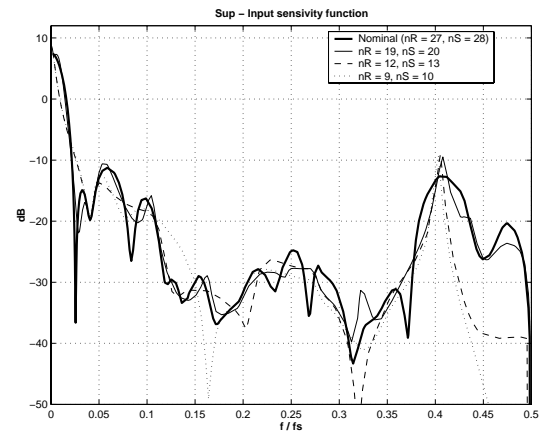


Figure 8: Input sensitivity for the active suspension (controller reduction using CLIM algorithm on simulated data)

5 Identification of reduced order controllers

5.1 Identification of reduced order controllers using simulated data (CLIM algorithm)

First, the CLIM direct identification method of a reduced order controller has been used, based on simulated data.

The frequency characteristics of the sensitivity functions (S_{yp}, S_{up}) for the nominal controller (K_n) with $n_R = 27, n_S = 28$, and for three reduced order controllers: K_1 with $n_R = 19, n_S = 20$, K_2 with $n_R = 12, n_S = 13$ and K_3 with $n_R = 9, n_S = 10$ are shown in figures 7 and 8 respectively (a fixed part $H_R = 1 + q^{-1}$ has been imposed in the reduced order controllers).

Note that the reduced controller K_2 corresponds to the complexity of the pole placement controller with the fixed part H_R . Controller K_3 has a complexity lower than that corresponding to the pole placement.

To illustrate the performances of the resulting controllers (K_n, K_1, K_2 and K_3) on the real system, the spectral

density of the residual acceleration in open and in closed loop is shown in Fig. 9. The primary source of vibration (shaker's excitation) is a PRBS. The characteristics obtained in closed loop operation with the four controllers are compared with those corresponding to the open loop operation (the interesting frequency range is 0 to $0.25f_s$ (200 Hz)). One can see that the performances of the reduced order controllers are close to that of the nominal controller and all achieve a significant reduction of the vibrations around the first vibration mode of the plant model.

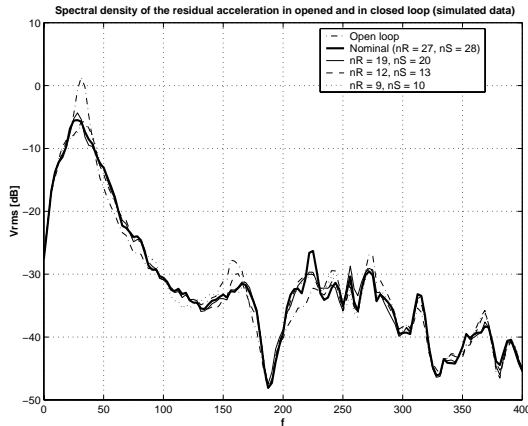


Figure 9: Spectral density of the residual acceleration in open and in closed loop (controller reduction using CLIM algorithm on simulated data)

5.2 Identification of reduced order controllers using real time data (CLIM algorithm)

The frequency characteristics of the sensitivity functions and of the reduced order controllers are very close to those of the reduced order controllers obtained with simulated data (the corresponding figures have been omitted). The spectral density of the residual acceleration in open and in closed loop is shown in Fig. 10.

Comparing the spectral density of the residual acceleration given in Figs. 9 and 10 one can see that the performances of the reduced order controllers using either simulated data or real data are very close. This can be explained by the quality of the identified model used for controller reduction.

5.3 Identification of reduced order controllers using CLIM algorithm with filtered r (simulated data)

It was verified that CLIM algorithm with filtered r through \hat{G} gives a preference to the minimization of the error between the output sensitivity functions while CLIM algorithm gives a preference to the minimization of the error between the input sensitivity functions.

Despite small differences in the achieved spectral density of the residual acceleration with respect to those obtained using CLIM algorithm, all reduced controllers

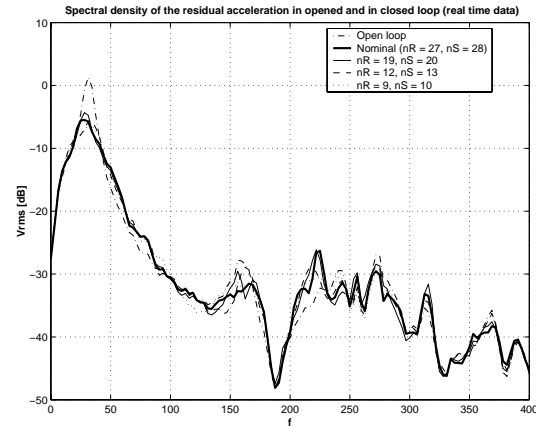


Figure 10: Spectral density of the residual acceleration in open and in closed loop (controller reduction using CLIM algorithm on real-time data)

give performances very close to those of the nominal controller.

Conclusions

Algorithms proposed in [5, 4] for direct closed loop identification of reduced order digital controllers have been experimentally tested on an active suspension system.

References

- [1] I.D.Landau, R. Lozano, and M. M'Saad. *Adaptive control*. Springer, London, 1997.
- [2] A. Karimi and I.D. Landau. Controller order reduction by direct closed loop identification (output matching). *IFAC Symp. ROCOND 2000*, Prague June 2000.
- [3] I.D. Landau and A. Karimi. Recursive algorithms for identification in closed loop - a unified approach and evaluation. *Automatica*, 33(8):1499–1523, 1997.
- [4] I.D. Landau and A. Karimi. Model estimation and controller reduction:dual closed loop identification problems. *submitted to CDC 2000*, Sydney Dec 2000.
- [5] I.D. Landau and A. Karimi. Direct closed loop identification of reduced order controllers (input matching). *IFAC Symp. SYSID 2000*, S. Barbara June 2000.
- [6] J. Langer and I.D. Landau. Combined pole placement/sensitivity function shaping method using convex optimization criteria. *Automatica*, 35:1111–1120, 1999.
- [7] G. Vinnicombe. Frequency domain uncertainty and the graph topology. *IEEE Trans. on Automatic Control*, 38:1571–1583, 1993.